Experimental Demonstration of Tripartite Entanglement and Controlled Dense Coding for Continuous Variables

Jietai Jing, Jing Zhang, Ying Yan, Fagang Zhao, Changde Xie, and Kunchi Peng

The State Key Laboratory of Quantum Optics and Quantum Optics Devices, Institute of Opto-Electronics, Shanxi University, Taiyuan, 030006, People's Republic of China

(Received 17 October 2002; published 23 April 2003)

A tripartite entangled state of bright optical field is experimentally produced using an Einstein-Podolsky-Rosen entangled state for continuous variables and linear optics. The controlled dense coding among a sender, a receiver, and a controller is demonstrated by exploiting the tripartite entanglement. The obtained three-mode "position" correlation and relative "momentum" correlation between the sender and the receiver, and thus the improvements of the measured signal to noise ratios of amplitude and phase signals with respect to the shot noise limit are 3.28 and 3.18 dB, respectively. If the mean photon number $\overline{n}$ equals 11 the channel capacity can be controllably inverted between 2.91 and 3.14. When $\overline{n}$ is larger than 1.0 and 10.52, the channel capacity of the controlled dense coding is predicted to exceed the ideal single channel capacity of coherent and squeezed state light communication, respectively.

DOI: 10.1103/PhysRevLett.90.167903 PACS numbers: 03.67.Hk, 03.65.Ud, 03.67.Mn, 42.50.Dv

Quantum entanglement shared by more than two parties is the essential base for developing quantum communication networks and quantum computation. The three-particle entangled states for discrete variables, also called Greenberger-Horne-Zeilinger (GHZ) states, have been proposed [1] and then experimentally realized [2,3]. The controlled dense coding (CDC) for discrete variables using a three-particle entangled state has been theoretically discussed [4]. Recently, under the motivation of the successful experiments on continuous-variable (CV) quantum teleportation [5] and quantum dense coding [6], the schemes demonstrating quantum teleportation network [7] and CDC [8] for CV using multipartite entanglement have been proposed. A necessary and sufficient condition for the separability of tripartite three-mode Gaussian states has been theoretically derived [9]. An experimentally accessible criterion for a GHZ-like state of CV has been given by van Loock and Braunstein [7]. A GHZ-like state is a three-mode momentum (position) eigenstate with total momentum $p_1 + p_2 + p_3 = 0$ (position $x_1 + x_2 + x_3 = 0$) and relative positions $x_i - x_j = 0$ $(i, j = 1, 2, 3)$ (momenta $p_i - p_j = 0$). In experiments using optical modes, the phase and amplitude quadratures of light fields correspond to the momentum and position components, respectively. If measured noise power spectra of total phase (amplitude) quadratures of three modes and relative amplitude (phase) quadratures are below the corresponding shot noise limit (SNL), we say the three optical modes are in a tripartite entangled state. So far to the best of our knowledge, the experimental report on the generation of multipartite entangled state for CV and its application has not been presented.

In this Letter we report the first experimental demonstration of quantum entanglement among more than two quantum systems with continuous spectra. The tripartite entangled state is produced by distributing a two-mode squeezed state light to three parties using linear optics. The obtained tripartite entangled optical beams are distributed to a sender (Alice), a receiver (Bob), and a controller (Claire), respectively. The information transmission capacity of the quantum channel between Alice and Bob is controlled by Claire. The channel capacity (CC) accomplished under Claire's help is always larger than that without her help. For large mean photon numbers ($\overline{n} > 10.52$), the CC of the CDC communication is predicted to exceed that of ideal squeezed state communication.

Figure 1 is the schematic of the experimental setup for tripartite entanglement generation and CDC. A semi-monolithic nondegenerate optical parameter amplifier (NOPA) involving an α-cut type-II KTP crystal and pumped by an intracavity frequency-doubled and frequency-stabilized Nd:YAP/KTP (potassium titanyl phosphate) laser serves as the initial bipartite entanglement source. The configuration and operation principle of this source have been described in detail in our previous

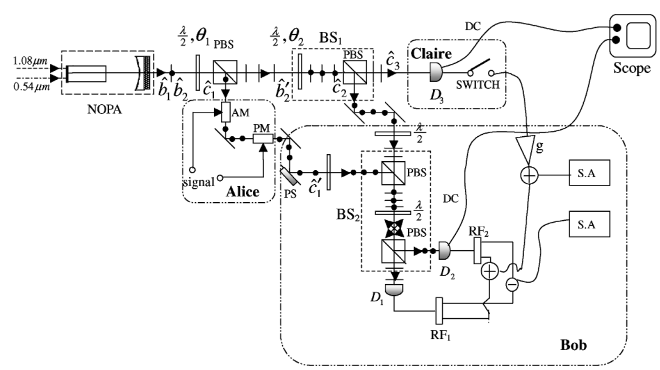

FIG. 1. Experimental setup for tripartite entanglement generation and controlled dense coding.

publications [6,10]. The output optical modes with horizontal and vertical polarizations $\hat{b}_1$ and $\hat{b}_2$ are a pair of bright Einstein-Podolsky-Rosen (EPR) entangled beams with anticorrelated amplitude quadratures and correlated phase quadratures [6]. The polarizations of $\hat{b}_1$ and $\hat{b}_2$ are rotated by a half-wave plate ($\lambda/2$), the optical axis of which is in $\theta_1 = 45° - \frac{1}{2}\arcsin[(\sqrt{2}-1)/\sqrt{6}]$ relative to the horizontal direction, and then the beams pass through a polarizing beam splitter (PBS) with horizontal and vertical polarizations. The output beam $\hat{b}_2'$ is split again by a 50/50 beam splitter (BS_1) consisting of a half-wave plate ($\lambda/2$) and a PBS to modes $\hat{c}_2$ and $\hat{c}_3$. In Ref. [8] we have proved theoretically that the modes $\hat{c}_1$, $\hat{c}_2$, and $\hat{c}_3$ are in a tripartite entangled state which is a "three-mode position eigenstate" with the quantum correlations of total position quadratures ($\hat{X}_{c_1}$, $\hat{X}_{c_2}$, and $\hat{X}_{c_3}$) and relative momentum quadratures ($\hat{Y}_{c_1}$, $\hat{Y}_{c_2}$, and $\hat{Y}_{c_3}$) (see Fig. 4 of Ref. [8] for the case of $r_2 = 0$). The outgoing tripartite entangled state is utilized to implement the CDC.

The entangled beams $\hat{c}_1$, $\hat{c}_2$, and $\hat{c}_3$ are sent to Alice, Bob, and Claire, respectively. Alice modulates two sets of classical signals on the amplitude and phase quadratures of her mode $\hat{c}_1$ by amplitude and phase modulators AM and PM. The modulations on mode $\hat{c}_1$ lead to a displacement of a_s:

$$\hat{c}\,'_1 = \hat{c}_1 + a_s, \tag{1}$$

where $a_s = X_s + iY_s$ is the sent signal via the quantum channel. The outgoing mode $\hat{c}_1'$ is sent to Bob who imposes a phase difference of $\pi/2$ between $\hat{c}_1'$ and himself at mode $\hat{c}_2$ with a phase shifter (PS), and then combines the two modes on BS_2. The two output beams from BS_2 are directly detected by photodiodes D_1 and D_2. The photocurrent of D_1 and D_2 is divided into two parts with power splitters RF1 and RF2, respectively. Through analogous calculation with Ref. [8] but taking into account the imperfect detection efficiency of the detectors ($\eta < 1$ for D_1, D_2, and D_3) and the nonzero losses of optical systems ($\xi_1 \neq 0$ for $\hat{c}_1$ and $\hat{c}_2$, $\xi_2 \neq 0$ for $\hat{c}_3$) the noise power spectra of the sum and difference photocurrents of $\hat{c}_1$ and $\hat{c}_2$ modes are expressed by [11]

$$\begin{aligned}\langle \delta^2 \hat{\imath}_+ \rangle &= \eta^2 \xi_1^2 \frac{e^{2r} + 8e^{-2r} - 9}{12} + 1 + \frac{1}{2} V_{X_s}, \\ \langle \delta^2 \hat{\imath}_- \rangle &= 3\eta^2 \xi_1^2 \frac{e^{-2r} - 1}{4} + 1 + \frac{1}{2} V_{Y_s},\end{aligned} \tag{2}$$

where r is the squeezing parameter of the EPR beams ($0 \leq r < \infty$), and V_{X_s} and V_{Y_s} are the fluctuation variances of the modulated signals (X_s, Y_s). Claire detects the amplitude quadrature of mode $\hat{c}_3$ with photodiode D_3 and sends the measured photocurrent to Bob. Bob displaces Claire's result on the sum photocurrent:

$$\begin{aligned}\hat{\imath}\,'_+ &= \hat{\imath}_+ + g\hat{\imath}_3 \\ &= \frac{\eta\xi_1}{\sqrt{2}}(\hat{X}_{c_1'} + \hat{X}_{c_2}) + g\eta\frac{\xi_2^2}{\xi_1}\hat{X}_{c_3} + \frac{\eta\sqrt{1-\xi_1^2}}{\sqrt{2}}(\hat{X}_{v_{c_1}} + \hat{X}_{v_{c_2}}) + \frac{\sqrt{1-\eta^2}}{2}(\hat{X}_{v_{D_1}} + \hat{Y}_{v_{D_1}} + \hat{X}_{v_{D_2}} - \hat{Y}_{v_{D_2}}) \\ &\quad + \frac{g\eta\xi_2^2\sqrt{1-\xi_2^2}}{\xi_1}\hat{X}_{v_{c_3}} + \frac{g\xi_2\sqrt{1-\eta^2}}{\xi_1}\hat{X}_{v_{D_3}} + \frac{1}{\sqrt{2}}X_s,\end{aligned} \tag{3}$$

where g describes gain at Bob for the transformation from Claire's photocurrent to Bob's sum photocurrent. The optimal gain for attaining the minimum variances of the sum photocurrent is

$$g_{\mathrm{opt}} = \frac{(e^{4r} + 3e^{2r} - 4)\eta^2\xi_1^2}{\sqrt{2}(e^{4r}\eta^2\xi_2^2 - 3e^{2r}\eta^2\xi_2^2 + 6e^{2r} + 2\eta^2\xi_2^2)}.$$

It is easy to be seen that for larger squeezing the optimum gain of the sum photocurrent is $g = \frac{1}{\sqrt{2}}$. For simplification and without losing generality, we take $g = \frac{1}{\sqrt{2}}$ in the following calculation and experiment, so the power fluctuation spectrum of sum photocurrent of three modes equals

$$\langle \delta^2 \hat{\imath}'_+ \rangle = \frac{1}{12}\left\{ e^{2r}\eta^2\left(\frac{\xi_2^2 - \xi_1^2}{\xi_1}\right)^2 + 2e^{-2r}\eta^2\left(\frac{\xi_2^2 + 2\xi_1^2}{\xi_1}\right)^2 - 3\left(\frac{\xi_2^4}{\xi_1^2}\eta^2 - 4 + 3\eta^2\xi_1^2 + 2\xi_2^2\eta^2 - 2\frac{\xi_2^2}{\xi_1^2}\right)\right\} + \frac{1}{2}V_{X_s}. \tag{4}$$

Figure 2(a) shows the measured noise power spectra of the amplitude sums $\langle \delta^2 \hat{\imath}'_+ \rangle$ (trace 3) and $\langle \delta^2 \hat{\imath}_+ \rangle$ (trace 2). The peak height of the modulated amplitude signal (X_s) on mode $\hat{c}_1$ at 2 MHz is 1.46 dBm higher than the noise background of $\langle \delta^2 \hat{\imath}'_+ \rangle$ (trace 3). Although the signal modulated on mode $\hat{c}_1$ is included in both $\langle \delta^2 \hat{\imath}'_+ \rangle$ and $\langle \delta^2 \hat{\imath}_+ \rangle$ and the peak height of the signal is the same (~ -96.88 dBm), in trace 2 the modulated signal is submerged in itself at the noise floor and cannot be observed due to the fact that the noise floor of $\langle \delta^2 \hat{\imath}_+ \rangle$ (~ -96.77 dBm) is higher than the height of the modulation signal. After the correction to the electronics noise floor (trace 4), the noise reductions of ($\hat{X}_{c_1} + \hat{X}_{c_2} + \hat{X}_{c_3}$) and ($\hat{X}_{c_1} + \hat{X}_{c_2}$) relative to SNL should actually be 3.28 and 1.19 dBm, respectively. Trace 2 in Fig. 2(b) is the

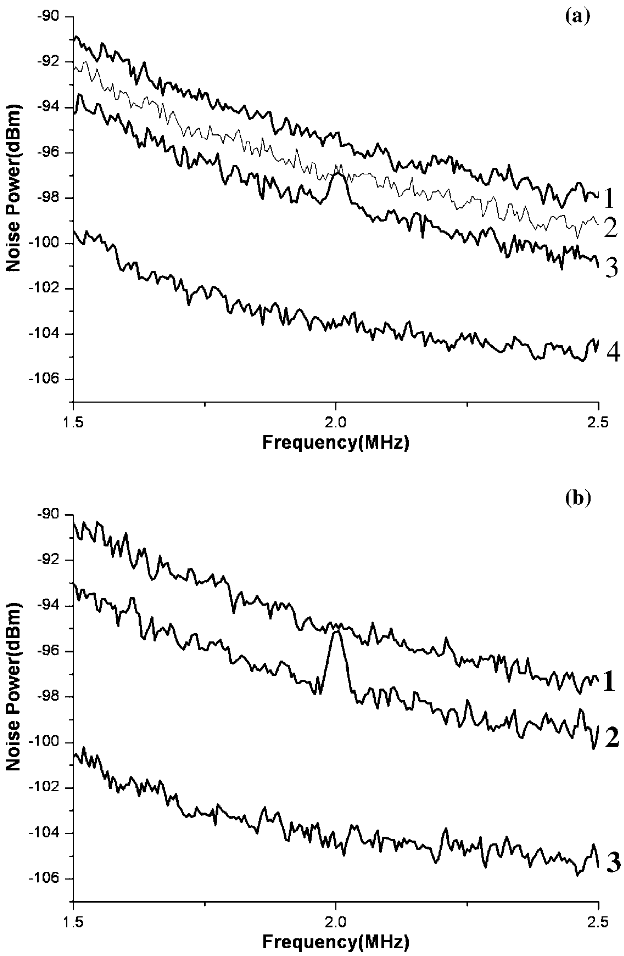

FIG. 2. (a) The noise power spectra of amplitude sums $\langle\delta^2\hat{\imath}'_+\rangle$ (trace 3) and $\langle\delta^2\hat{\imath}_+\rangle$ (trace 2), trace 1—shot noise limit (SNL), trace 4—electronics noise level (ENL), measured frequency range 1.5–2.5MHz, resolution bandwidth 30 KHz, video bandwidth 0.1 KHz. (b) The noise power spectra of phase difference $\langle\delta^2\hat{\imath}_-\rangle$ (trace 2), trace 1—SNL, trace 3—ENL, measured frequency range 1.5–2.5 MHz, resolution bandwidth 30 KHz, video bandwidth 0.1 KHz.

measured noise power spectrum of $(\hat{Y}_{c_1} - \hat{Y}_{c_2})$ which is 2.66 dBm below the SNL (trace 1). Accounting for the electronics noise (trace 3), it should be 3.18 dBm below the SNL actually. Figures 2(a) and 2(b) show that the noise power spectra of both $\langle\delta^2\hat{\imath}'_+\rangle$ and $\langle\delta^2\hat{\imath}_-\rangle$, i.e., both $(\hat{X}_{c_1} + \hat{X}_{c_2} + \hat{X}_{c_3})$ and $(\hat{Y}_{c_1} - \hat{Y}_{c_2})$, are below the corresponding SNL. According to the criteria of the GHZ-like state for CV mentioned above and the classification of five different entanglement classes given in Ref. [9], the modes $\hat{c}_1$, $\hat{c}_2$, and $\hat{c}_3$ constitute a tripartite entangled state classified in Class 1 of Ref. [9]. Substituting the measured noise power of $\langle\delta^2\hat{\imath}_+\rangle$, $\langle\delta^2\hat{\imath}'_+\rangle$, and $\langle\delta^2\hat{\imath}_-\rangle$ from Fig. 2 into Eqs. (2) and (4), we calculate the squeezing parameter $r_{\rm exp} = 0.674$ (5.85 dBm squeezing after the correction). The parameters $\langle\delta^2\hat{\imath}_+\rangle = 0.76$, $\langle\delta^2\hat{\imath}'_+\rangle = 0.47$, $\langle\delta^2\hat{\imath}_-\rangle = 0.48$, $\xi_1^2 = 98.7\%$, $\xi_2^2 = 93.7\%$, $\eta^2 = 95.0\%$ are taken in the calculation according to the experimental values.

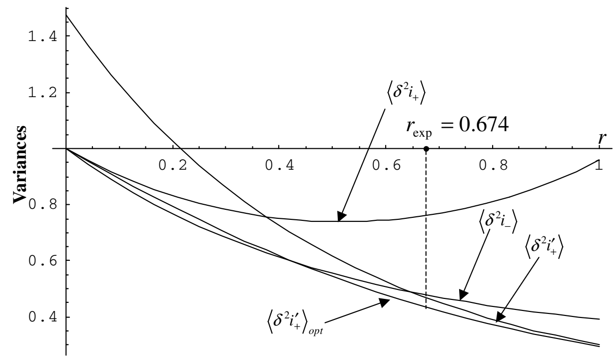

FIG. 3. The variances of amplitude sums $\langle\delta^2\hat{\imath}_+\rangle$, $\langle\delta^2\hat{\imath}'_+\rangle$, $\langle\delta^2\hat{\imath}'_+\rangle_{\rm opt}$, and phase difference $\langle\delta^2\hat{\imath}_-\rangle$ versus the squeezing parameter r with beam propagation efficiency $\xi_1^2 = 98.7\%$, $\xi_2^2 = 93.7\%$, and the quantum efficiency of detector $\eta^2 = 95.0\%$.

Figure 3 shows the functions of the normalized fluctuation variances of $\langle\delta^2\hat{\imath}_-\rangle$, $\langle\delta^2\hat{\imath}_+\rangle$, and $\langle\delta^2\hat{\imath}'_+\rangle$ versus the squeezing parameter r, where ξ_1, ξ_2, η, and $g = \frac{1}{\sqrt{2}}$ are the values for the experimental system. $\langle\delta^2\hat{\imath}'_+\rangle_{\rm opt}$ is the fluctuation variance of the amplitude sum of three modes when the optimal gain $g_{\rm opt}$ is applied. We can see the difference between $\langle\delta^2\hat{\imath}'_+\rangle_{\rm opt}$ and $\langle\delta^2\hat{\imath}'_+\rangle$ is quite small (0.035) for the experimental squeezing $r_{\rm exp} = 0.674$, and the difference tends to zero for larger r. $\langle\delta^2\hat{\imath}'_+\rangle$ is smaller than $\langle\delta^2\hat{\imath}_+\rangle$ and increasing r, $\langle\delta^2\hat{\imath}_+\rangle$ increases, but $\langle\delta^2\hat{\imath}'_+\rangle$ decreases. It means that the noise power of the amplitude sum of three modes $\hat{c}_1$, $\hat{c}_2$, and $\hat{c}_3$ is smaller than that of the two modes $\hat{c}_1$ and $\hat{c}_2$, which is the result of quantum correlation among the three amplitude quadratures $\hat{X}_{c_1}$, $\hat{X}_{c_2}$, and $\hat{X}_{c_3}$. In our experiment ($r_{\rm exp} = 0.674$) $\langle\delta^2\hat{\imath}'_+\rangle$ is 0.29 lower than $\langle\delta^2\hat{\imath}_+\rangle$. There is indeed quantum entanglement in the obtained three modes since if $\hat{c}_1$, $\hat{c}_2$, and $\hat{c}_3$ modes were classical light fields without entanglement, the amplitude fluctuation of the sum of the three modes would necessarily be larger than that of the sum of $\hat{c}_1$ and $\hat{c}_2$ modes.

Following the theoretical calculations on the quantum CC for dense coding in Refs. [8,11,12] we calculate the CC of the presented experimental system. The CC with and without Claire's help can be deduced from Eqs. (2) and (4):

$$C_{n-c}^{\rm dense} = \frac{1}{2}\ln\left[\left(1 + \frac{\sigma^2}{\langle\delta^2\hat{\imath}_-\rangle}\right)\left(1 + \frac{\sigma^2}{\langle\delta^2\hat{\imath}_+\rangle}\right)\right],$$
$$C_{c}^{\rm dense} = \frac{1}{2}\ln\left[\left(1 + \frac{\sigma^2}{\langle\delta^2\hat{\imath}_-\rangle}\right)\left(1 + \frac{\sigma^2}{\langle\delta^2\hat{\imath}'_+\rangle}\right)\right], \qquad (5)$$

where σ^2 is the average value of the signal photon number and the mean photon number per mode $\bar{n} = \sigma^2 + \sinh^2 r$ [8,13]. The dependences of the CC for ideal single mode coherent state $[C^{ch} = \ln(1 + \bar{n})]$ and squeezing state $[C^{sq} = \ln(1 + 2\bar{n})]$ [8,12,13] on the mean photon number $\bar{n}$ are given in Fig. 4 to compare with that of CDC with

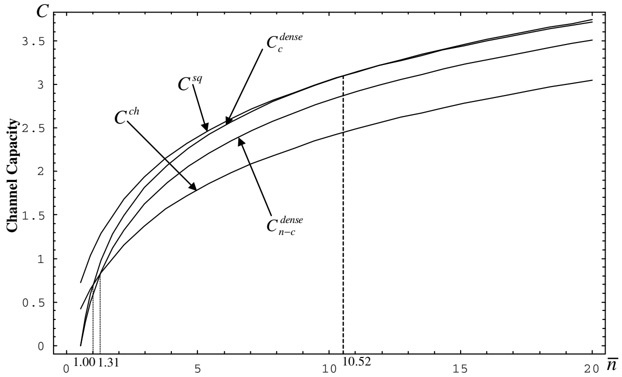

FIG. 4. CC for the controlled dense coding with (C_c^{dense}) and without (C_{n-c}^{dense}) Claire's help, single-mode coherent state with heterodyne detection, and squeezed state (C^{sq}) communication. The parameters are same as Fig. 3.

(C_c^{dense}) and without (C_{n-c}^{dense}) Claire's help according to Eq. (5) and taking the experimental parameters. For the given squeezing ($r_{\text{exp}} = 0.674$), when the mean photon number $\overline{n}$ is larger than 1.00 (1.31), C_c^{dense} (C_{n-c}^{dense}) will exceed C^{ch} and when $\bar{n} > 10.52$, C_c^{dense} will be larger than C^{sq}. By increasing the average signal photon number σ^2, the CC of quantum dense coding can be improved [12]. The CC with the help of Claire (C_c^{dense}) is always larger than that without her help (C_{n-c}^{dense}) which is the result of the signal to noise ratio improvement due to using three-partite entanglement [12]. For example, when $\overline{n} = 11$, the CC of the presented system can be controllably inverted between 2.91 and 3.14.

In conclusion, we experimentally obtained bright tripartite entangled state light and accomplished the quantum controlled dense coding for the continuous variables. We deduced the formulas designating the tripartite entanglement in which the influences of imperfect detection efficiency and the losses of optical system are included. The experiment shows that using the accessible entanglement of optical modes the CC of the CDC can exceed that of coherent state and squeezed state communication when the signal photon number is larger than a certain value. The mature technique of optical parametric amplification, the simple linear optical system and the direct measurement for the Bell state are used in the presented scheme; thus the experimental implementation is significantly simplified relative to the systems using the balanced homodyne detectors [5,7].

This research was supported by the National Fundamental Research Natural Science Foundation of China (Grant No. 2001CB309304), the National Natural Science Foundation of China(Grants No. 60238010 and No. 60178012), and the Shanxi Province Young Science Foundation (Grant No. 20021014).

[1] D. M. Greenberger *et al.*, Am. J. Phys. **58**, 1131 (1990).
[2] D. Bouwmeester *et al.*, Phys. Rev. Lett. **82**, 1345 (1999).
[3] R. Laflamme *et al.*, Philos. Trans. R. Soc. London A **356**, 1941 (1998).
[4] J. C. Hao, C. F. Li, and G. C. Guo, Phys. Rev. A **63**, 054301 (2001).
[5] A. Furusawa, J. L. Sorensen, S. L. Braunstein, C. A. Fuchs, H. J. Kimble, and E. S. Polzik, Science **282**, 706 (1998).
[6] X. Li, Q. Pan, J. Jing, J. Zhang, C. Xie, and K. Peng, Phys. Rev. Lett. **88**, 047904 (2002).
[7] P. van Loock and S. L. Braunstein, Phys. Rev. Lett. **84**, 3482 (2000).
[8] J. Zhang, C. Xie, and K. Peng, Phys. Rev. A **66**, 032318 (2002).
[9] G. Giedke, B. Kraus, M. Lewenstein, and J. I. Cirac, Phys. Rev. A **64**, 052303 (2001).
[10] Y. Zhang, H. Wang, X. Li, J. Jing, C. Xie, and K. Peng, Phys. Rev. A **62**, 023813 (2000).
[11] J. Zhang and K. Peng, Phys. Rev. A **62**, 064302 (2000).
[12] T. C. Ralph and E. H. Huntington, Phys. Rev. A **66**, 042321 (2002).
[13] S. L. Braunstein and H. J. Kimble, Phys. Rev. A **61**, 042302 (2000).